PHYSICAL REVIEW B **89**, 220408(R) (2014)

Phase diagram of a frustrated spin-$\frac{1}{2}$ J_1-J_2 XXZ model on the honeycomb lattice

P. H. Y. Li,[1,*] R. F. Bishop,[1,†] and C. E. Campbell[2]

[1]*School of Physics and Astronomy, Schuster Building, University of Manchester, Manchester M13 9PL, United Kingdom*

[2]*School of Physics and Astronomy, University of Minnesota, 116 Church Street SE, Minneapolis, Minnesota 55455, USA*

(Received 8 April 2014; revised manuscript received 26 May 2014; published 24 June 2014)

We study the zero-temperature ($T = 0$) ground-state (GS) properties of a frustrated spin-half J_1^{XXZ}–J_2^{XXZ} model on the honeycomb lattice with nearest-neighbor and next-nearest-neighbor interactions with exchange couplings $J_1 > 0$ and $J_2 \equiv \kappa J_1 > 0$, respectively, using the coupled cluster method. Both interactions are of the anisotropic XXZ type. We present the $T = 0$ GS phase diagram of the model in the ranges $0 \leqslant \Delta \leqslant 1$ of the spin-space anisotropy parameter and $0 \leqslant \kappa \leqslant 1$ of the frustration parameter. A possible quantum spin-liquid region is identified.

DOI: 10.1103/PhysRevB.89.220408 PACS number(s): 75.10.Jm, 75.10.Kt, 75.30.Kz, 75.30.Gw

Frustrated spin-half ($s = \frac{1}{2}$) antiferromagnets with nearest-neighbor (NN) $J_1 > 0$ and competing next-nearest-neighbor (NNN) $J_2 > 0$ exchange couplings on the honeycomb lattice have attracted a great deal of interest in recent years. These have included the two specific cases where both couplings have either an isotropic Heisenberg (XXX) form (see, e.g., Refs. [1–16], and references cited therein) or an isotropic XY (XX) form (see, e.g., Refs. [17–23]). Although the classical ($s \to \infty$) versions of these two models have identical zero-temperature ($T = 0$) ground-state (GS) phase diagrams [1,2], their $s = \frac{1}{2}$ counterparts differ in significant ways. Furthermore, there is not yet a complete consensus on the GS phase orderings for either model in the range $0 \leqslant \kappa \leqslant 1$ of the frustration parameter $\kappa \equiv J_2/J_1$.

Whereas both classical ($s \to \infty$) models have Néel ordering for $\kappa < \kappa_{\rm cl} = \frac{1}{6}$, the spin-$\frac{1}{2}$ models both seem to retain Néel order out to larger values $\kappa_{c_1} \approx 0.2$, consistent with the fact that quantum fluctuations generally favor collinear over noncollinear ordering. The degenerate family of spiral states that form the classical GS phase for all values $\kappa > \kappa_{\rm cl}$ is very fragile against quantum fluctuations, and there is broad agreement that neither $s = \frac{1}{2}$ model has a stable GS phase with spiral ordering for any value of κ in the range $0 \leqslant \kappa \leqslant 1$.

The most interesting, and also most uncertain, regime for both $s = \frac{1}{2}$ models is when $0.2 \lesssim \kappa \lesssim 0.4$. For the XXX model the Néel order that exists for $\kappa < \kappa_{c_1} \approx 0.2$ is predicted by different methods to give way either to a GS phase with plaquette valence-bond crystalline (PVBC) order [6,7,10–14] or to a quantum spin-liquid (QSL) state [5,9,15,16] in the range $\kappa_{c_1} < \kappa < \kappa_{c_2} \approx 0.4$. By contrast, for the XX model the Néel xy planar [N(p)] ordering that exists for $\kappa < \kappa_{c_1}$ is predicted by different methods to yield either to a GS phase with Néel z-aligned [N(z)] order [19,23] or to a QSL state [17,20] in a corresponding range $\kappa_{c_1} < \kappa < \kappa_{c_2}$. There is broad agreement for both models that for (1 >) $\kappa > \kappa_{c_2}$ there is a strong competition to form the GS phase between states with collinear Néel-II xy planar [N-II(p)] and staggered dimer valence-bond crystalline (SDVBC) forms of order, which lie very close in energy. The (threefold-degenerate) Néel-II states, which break the lattice rotational symmetry, are ones in which NN pairs of spins are parallel along one of the three equivalent honeycomb directions and antiparallel along the other two. Some methods favor a further quantum critical point (QCP) at $\kappa_{c_3} > \kappa_{c_2}$, at which a transition occurs between GS phases with SDVBC ordering for $\kappa_{c_2} < \kappa < \kappa_{c_3}$, possibly mixed with N-II(p) ordering over all or part of the region, and N-II(p) ordering alone for $\kappa > \kappa_{c_3}$.

The intriguing differences between the two models motivate us to consider the so-called J_1^{XXZ}–J_2^{XXZ} model that interpolates between them. It is shown schematically in Fig. 1(a) and is described by the Hamiltonian

$$H = J_1 \sum_{\langle i,j \rangle} \left(s_i^x s_j^x + s_i^y s_j^y + \Delta s_i^z s_j^z \right) + J_2 \sum_{\langle\langle i,k \rangle\rangle} \left(s_i^x s_k^x + s_i^y s_k^y + \Delta s_i^z s_k^z \right), \quad (1)$$

where $\langle i,j \rangle$ and $\langle\langle i,k \rangle\rangle$ indicate NN and NNN pairs of spins, respectively, and $\mathbf{s}_i = (s_i^x, s_i^y, s_i^z)$ is the spin operator on lattice site i. We shall study the $T = 0$ GS phase diagram for the spin-$\frac{1}{2}$ Hamiltonian of Eq. (1) on the honeycomb lattice in the range $0 \leqslant \Delta \leqslant 1$ of the spin anisotropy parameter that spans from the XX model (with $\Delta = 0$) to the XXX model (with $\Delta = 1$), and in the range $0 \leqslant \kappa \leqslant 1$ of the frustration parameter. Henceforth we put $J_1 \equiv 1$ to set the overall energy scale. We note that both exact diagonalization (ED) of small finite lattices and density-matrix renormalization group (DMRG) studies of the XX model in particular find it especially difficult to distinguish the N-II(p) and SDVBC phases in the regime $\kappa > \kappa_{c_2}$ in the thermodynamic limit, $N \to \infty$, where N is the number of lattice sites. For this reason it is particularly suitable to use a size-extensive method such as the coupled cluster method (CCM) that works from the outset in the $N \to \infty$ limit.

We first describe some key features of the CCM and refer the reader to Refs. [11,12,23–31] for more details. Any CCM calculation starts with the choice of a suitable model (or reference) state $|\Phi\rangle$. Here we use each of the N(p), N(z), and N-II(p) states shown schematically in Figs. 1(b)–1(d). In order to treat each lattice site on an equal footing we passively rotate each spin in each model state, so that in its own local spin-coordinate frame it points downwards (i.e., along the local negative z axis). In these local spin coordinates every model state thus takes the universal form $|\Phi\rangle = |\downarrow\downarrow\downarrow \cdots \downarrow\rangle$ and the Hamiltonian has to be rewritten accordingly. The exact GS energy eigenket, $|\Psi\rangle$,

*peggyhyli@gmail.com

†raymond.bishop@manchester.ac.uk

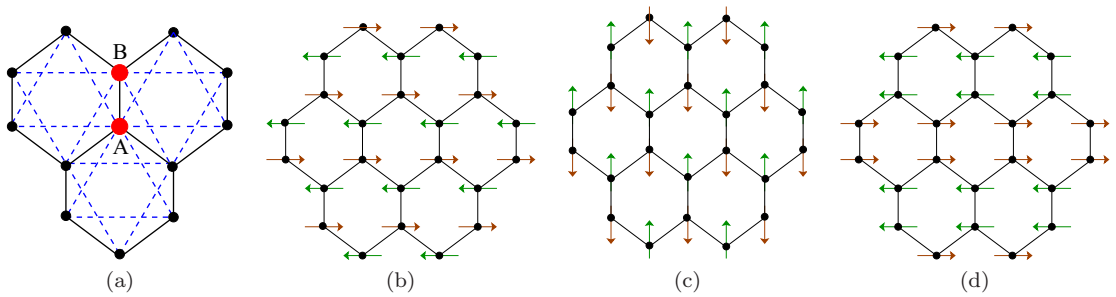

FIG. 1. (Color online) The J_1^{XXZ}–J_2^{XXZ} model on the honeycomb lattice, showing (a) the bonds ($J_1 \equiv$ ——; $J_2 \equiv$ – – –) and the two sites (●) A and B of the unit cell; (b) the Néel planar, N(p), state; (c) the Néel z-aligned, N(z), state; and (d) the Néel-II planar, N-II(p), state. The arrows represent the directions of the spins located on lattice sites ●.

with $H|\Psi\rangle = E|\Psi\rangle$, is now expressed in the exponentiated form, $|\Psi\rangle = e^S|\Phi\rangle$, where the creation correlation operator S is written as $S = \sum_{I\neq 0} \mathcal{S}_I C_I^+$, with $C_0^+ \equiv 1$, the identity operator. The corresponding GS energy eigenbra, $\langle\tilde{\Psi}|$, where $\langle\tilde{\Psi}|H = E\langle\tilde{\Psi}|$, is written as $\langle\tilde{\Psi}| = \langle\Phi|\tilde{S}e^{-S}$, where $\tilde{S} = 1 + \sum_{I\neq 0} \tilde{\mathcal{S}}_I C_I^-$, and $C_I^- \equiv (C_I^+)^\dagger$. The states obey the normalization conditions $\langle\tilde{\Psi}|\Psi\rangle = \langle\Phi|\Psi\rangle = \langle\Phi|\Phi\rangle = 1$ and the relations $\langle\Phi|C_I^+ = 0 = C_I^-|\Phi\rangle, \forall I \neq 0$, which ensure that $|\Phi\rangle$ is a fiducial vector with respect to the complete set of multispin creation operators $\{C_I^+\}$. In the local spin-coordinate frames, C_I^+ also takes a universal form, $C_I^+ \to s_{l_1}^+ s_{l_2}^+ \cdots s_{l_n}^+$, a product of single-spin raising operators, $s_l^+ \equiv s_l^x + i s_l^y$, where the set-index $I \to \{l_1, l_2, \cdots, l_n;\ n = 1,2,\cdots,2sN\}$. The set of multispin correlation coefficients $\{\mathcal{S}_I, \tilde{\mathcal{S}}_I\}$ is determined by requiring that the energy expectation value $\bar{H} = \bar{H}\{\mathcal{S}_I, \tilde{\mathcal{S}}_I\} \equiv \langle\Phi|\tilde{S}e^{-S}He^S|\Phi\rangle$ is a minimum. The GS magnetic order parameter is defined as $M \equiv -\frac{1}{N}\langle\tilde{\Psi}|\sum_{k=1}^N s_k^z|\Psi\rangle$, the average local on-site magnetization, with respect to the local (rotated) spin coordinates.

The *only* approximation now made in the CCM is to truncate the set of indices $\{I\}$ in the expansions of the correlation operators S and $\tilde{S}$. We use here the well-studied (lattice-animal-based subsystem) LSUBm scheme [11,12,23,28–31] in which, at the mth level of approximation, one retains all multispin-flip configurations $\{I\}$ defined over no more than m contiguous lattice sites. Such cluster configurations are defined to be contiguous if every site is NN to at least one other. The number, N_f, of such fundamental configurations is reduced by exploiting the space- and point-group symmetries and any conservation laws that pertain to the Hamiltonian and the model state being used. Even so, N_f increases rapidly with increasing LSUBm truncation index m, and it becomes necessary to use massive parallelization together with supercomputing resources [29,32]. For example, we have finally $N_f = 818\,300$ for the N-II(p) reference state at the LSUB12 level.

Finally, we extrapolate the "raw" LSUBm results to the limit $m \to \infty$ where the CCM becomes exact. For the GS energy per spin, $e \equiv E/N$, we employ the well-tested extrapolation scheme [11,12,23,30,31] $e(m) = e_0 + e_1 m^{-2} + e_2 m^{-4}$, in which we use results with $m = \{6,8,10,12\}$ for the N(p) and N-II(p) states taken as model state, and with $m = \{4,6,8,10\}$ for the N(z) state. For the magnetic order parameter of systems near a QCP an appropriate extrapolation rule is the "leading power-law" scheme [12,23], $M(m) = c_0 + c_1(1/m)^{c_2}$, which we use here for the LSUBm results based on the N(z) state with $m = \{4,6,8,10\}$. An alternative well-tested scheme for systems with strong frustration or where the order in question is zero or close to zero [11,12,23] is $M(m) = d_0 + d_1 m^{-1/2} + d_2 m^{-3/2}$, when the leading exponent c_2 above has been empirically found to be close to 0.5, as is the case here for results based on both the N(p) and N-II(p) model states with $m = \{6,8,10,12\}$.

Our corresponding extrapolated (LSUB∞) results for the GS energy per spin and the order parameter are shown in Figs. 2 and 3. In each case we present three curves for each value of the anisotropy parameter Δ shown, based in turn on the N(p), N(z), and N-II(p) model states. All of the curves in Fig. 2 display termination points, viz., an upper one for the N(p) curves, a lower one for the N-II(p) curves, and one of each type for the N(z) curves. In each case they correspond to the points of the respective LSUBm approximations with the highest value of m, beyond which real solutions for $\{\mathcal{S}_I\}$ cease to exist. Such termination points of LSUBm solutions are manifestations of a

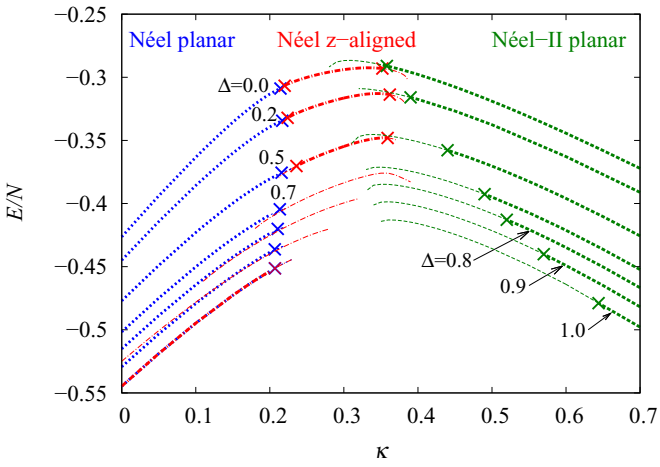

FIG. 2. (Color online) The GS energy per spin E/N versus the frustration parameter $\kappa \equiv J_2/J_1$ for the spin-$\frac{1}{2}$ J_1^{XXZ}–J_2^{XXZ} model on the honeycomb lattice (with $J_1 = 1$), for various values of the anisotropy parameter $\Delta = 0.0,0.2,0.5,0.7,0.8,0.9,1.0$ (from top to bottom, respectively). We show extrapolated CCM LSUB∞ results (see text for details) based on the Néel planar, Néel z-aligned, and Néel-II planar model states, respectively. The times (×) symbols mark the points where the respective extrapolations for the order parameter have $M \to 0$, and the unphysical portions of the solutions are shown by thinner lines (see text for details).

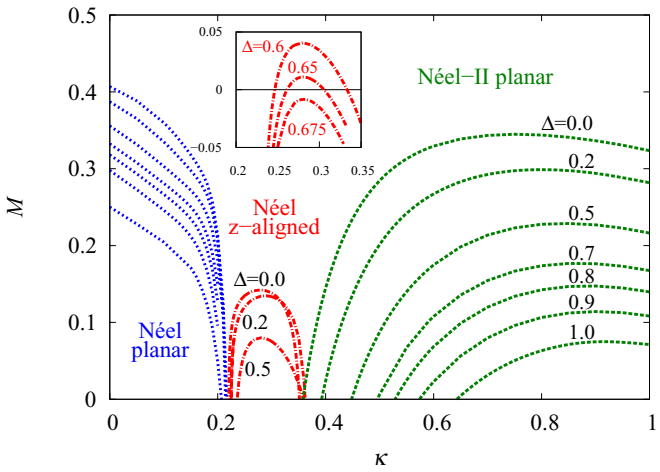

FIG. 3. (Color online) The GS magnetic order parameter M versus the frustration parameter $\kappa \equiv J_2/J_1$ for the spin-$\frac{1}{2}$ J_1^{XXZ}–J_2^{XXZ} model on the honeycomb lattice (with $J_1 > 0$) for various values of the anisotropy parameter $\Delta = 0.0, 0.2, 0.5, 0.7, 0.8, 0.9, 1.0$ (from top to bottom, respectively). We show extrapolated CCM LSUB∞ results (see text for details) based on the Néel planar, Néel z-aligned, and Néel-II planar states as CCM model states, respectively.

corresponding QCP in the system, beyond which the order associated with the model state under study melts (see, e.g., Refs. [11,12,23,30]). We find that as the index m is increased the range of values of κ for which the respective LSUBm equations have real solutions becomes narrower, such that as $m \to \infty$ each termination point becomes the corresponding exact QCP. Real LSUBm solutions with a finite value of m can thus also exist in regions where the corresponding order is destroyed (viz., where $M < 0$). We show in Fig. 2 by times ($\times$) symbols those points on the respective curves where $M = 0$ (as determined from the corresponding extrapolated LSUB∞ values shown in Fig. 3). We also denote in Fig. 2 by thinner lines those portions of the curves which are "unphysical" in the sense that $M < 0$, as opposed to the corresponding "physical" regions where $M > 0$, which are denoted by the thicker portions.

Figures 2 and 3 show that (a) N(p) order is present below a lower critical value $0 < \kappa < \kappa_{c_l}(\Delta)$, for all values of Δ, where $\kappa_{c_l}(\Delta) \approx 0.21$; (b) N($z$) order is present within a relatively narrow range of values around $\kappa \approx 0.3$ for all values $\Delta \lesssim 0.66$ and is absent for $\Delta \gtrsim 0.66$; (c) N-II(p) order is present above some upper critical value, (1 >) $\kappa > \kappa_{c_u}(\Delta)$, where $\kappa_{c_u}(\Delta)$ increases monotonically with Δ, (d) whereas the GS phases with N(p) and N(z) order present seem to meet at $\kappa_{c_l}(0)$ for $\Delta = 0$, a very narrow region of a GS phase with neither of these orderings opens up between them as Δ is increased; and (e) similarly, whereas the GS phases with N(z) and N-II(p) order seem to meet at $\kappa_{c_u}(0)$ for $\Delta = 0$, a phase with neither order opens between them as Δ is increased.

From our previous results at $\Delta = 0$ [23] and $\Delta = 1$ [11,12] and those of others, a possible phase for that mentioned under item (e) above is one with SDVBC ordering. A convenient way to test for the susceptibility of a candidate GS phase built on a specific CCM model state is to consider its response to an imposed field operator, $F = \delta\,\hat{O}$, added to our Hamiltonian of Eq. (1), where δ is a (positive) infinitesimal and the operator $\hat{O}$ now promotes SDVBC order ($\hat{O}_d$), as illustrated in Fig. 4. The corresponding perturbed energy per spin, $e(\delta) \equiv E(\delta)/N$, is calculated at various CCM LSUBm orders of approximation and used to calculate the respective susceptibility, $\chi \equiv -\partial^2 e(\delta)/\partial\delta^2|_{\delta=0}$ (and see Refs. [11,12,23] for more details). The GS phase becomes unstable against the imposed form of order whenever $1/\chi \to 0$. The results are extrapolated to the LSUB∞ limit using the "leading power-law" scheme, $\chi^{-1} \to x_0 + x_1 m^{-\nu}$. We show LSUB$\infty$ extrapolations based on the N-II(p) model state in Fig. 4, using this scheme with LSUBm results $m = \{4,6,8\}$, for various values of Δ.

Figure 4 shows that the locus of the lower critical values of κ at which SDVBC order appears is very insensitive to the value of Δ for all $\Delta \gtrsim 0.1$, taking the almost constant value $\kappa \approx 0.38$. Very interestingly, the locus of such SDVBC critical points meets the corresponding locus of critical values above which N-II(p) order appears [defined as the corresponding points $\kappa(\Delta)$ at which $M = 0$ for the N-II(p) state, as taken from Fig. 3] at just the value $\Delta \approx 0.1$. For values $\Delta \lesssim 0.1$, Fig. 4 shows that a region opens up in which both SDVBC and N-II(p) forms of order seem to coexist over a narrow range of values of κ, before N-II(p) order dominates for higher values of κ. This "mixed" region is denoted as M in the phase diagram shown in Fig. 5.

We also show in Fig. 5 the regions of stability of the N(z) and N(p) phases, taken from Fig. 3 as the corresponding regions in which the respective magnetic order parameters M take positive values.

A particularly interesting region in the phase diagram is the remaining one outside the region of N(z) stability and between

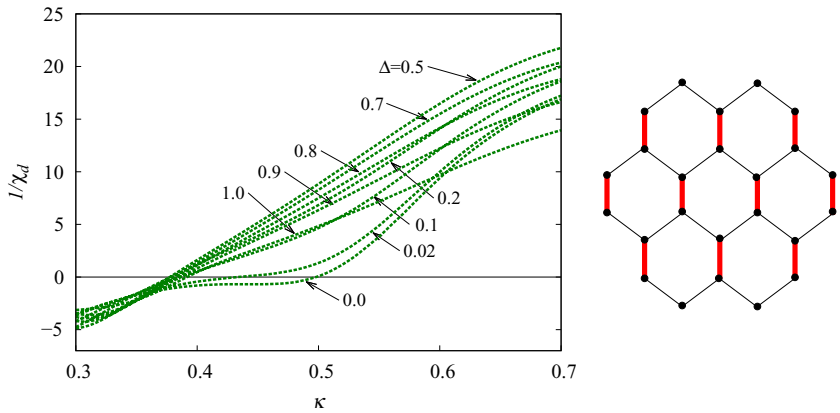

FIG. 4. (Color online) Left: The inverse staggered dimer susceptibility, $1/\chi_d$, versus the frustration parameter, $\kappa \equiv J_2/J_1$, for the spin-$\frac{1}{2}$ J_1^{XXZ}–J_2^{XXZ} model on the honeycomb lattice (with $J_1 = 1$) for various values of the anisotropy parameter Δ. We show extrapolated CCM LSUB∞ results (see text for details) based on the Néel-II planar state as CCM model state. Right: The field $F \to \delta\,\hat{O}_d$ for the staggered dimer susceptibility, χ_d. Thick (red) and thin (black) lines correspond respectively to strengthened and unaltered NN exchange couplings, where $\hat{O}_d = \sum_{\langle i,j\rangle} a_{ij}(s_i^x s_j^x + s_i^y s_j^y + \Delta s_i^z s_j^z)$, and the sum runs over all NN bonds, with $a_{ij} = +1$ and 0 for thick (red) lines and thin (black) lines, respectively.

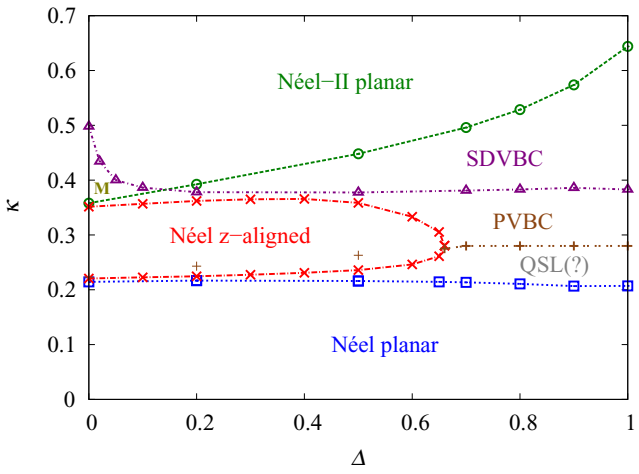

FIG. 5. (Color online) Phase diagram for the spin-$\frac{1}{2}$ J_1^{XXZ}–J_2^{XXZ} model on the honeycomb lattice (with $J_1 > 0$ and $\kappa \equiv J_2/J_1 > 0$) in the window $0 \leqslant \kappa \leqslant 1$ and $0 \leqslant \Delta \leqslant 1$, as obtained by a CCM analysis. The phase in the region marked "M" has both SDVBC and Néel-II planar order. See text for details.

the two curves $\kappa \approx 0.21$ [below which N(p) order is stable] and $\kappa \approx 0.38$ [above which SDVBC and/or N-II(p) order is stable], both curves being almost independent of Δ.

For the *XXX* model (viz., $\Delta = 1$) it remains open as to whether the GS phase in this region has PVBC order [6,7,10–14] or is a QSL state [5,9,16]. Of particular interest in this context is a recent DMRG study [15] of the *XXX* model that claimed to find solid evidence of (weak) PVBC order, in the thermodynamic ($N \to \infty$) limit, in the range $0.26 \lesssim \kappa \lesssim 0.35$, but which excluded (in the same limit) in the range $0.22 \lesssim \kappa \lesssim 0.26$ immediately above the Néel-ordered regime both magnetic (spin) and valence-bond orderings, consistent with a possible QSL phase. This result is also in broad agreement with our own earlier CCM findings [11], as we discuss below.

We have now also tested the stability of the N(p) phase against PVBC ordering by calculating the corresponding extrapolated inverse plaquette susceptibility, χ_p^{-1} (see, e.g., Ref. [11]), based on the N(p) model state and LSUB*m* results with $m = \{4,6,8\}$. The corresponding LSUB∞ points at which $\chi_p^{-1} \to 0$ are shown in Fig. 5 by the plus (+) symbols. Based on such results we tentatively identify the PVBC and QSL regions indicated in Fig. 5. The fact that the + symbols for $\Delta \lesssim 0.66$ do not fall precisely on the lower stability boundary of the N(z) regime may be an indication of the error bars associated with the PVBC boundary points. These would be reduced by including higher-order LSUB*m* results in the extrapolations. The entire PVBC and SDVBC regimes would more definitively be confirmed by performing calculations of χ_p^{-1} and χ_d^{-1} based on the N-II(p) state, to confirm their respective upper boundaries. Such LSUB∞ extrapolations based on the N-II(p) state are technically more difficult to make, however, and more definitive evidence awaits higher-order LSUB*m* calculations. In their absence we cannot exclude QSL behavior also in the regime between the N(z) and SDVBC phases for $\Delta \lesssim 0.66$.

In our earlier CCM analysis of the *XXX* model [11] we noted the possibility that the transition from the N(p) phase to the PVBC phase in that model might be via an intermediate phase, now identified here as a tentative QSL phase. Our best estimate then was that such an intermediate phase should be restricted to a region $\kappa_{c_1} < \kappa < \kappa'_{c_1}$. The value of κ_{c_1} was very accurately obtained, as $\kappa_{c_1} = 0.207(3)$, from the point where Néel order vanishes, and is identical to that shown in Fig. 5 for the boundary between the N(p) and potential QSL phases. The accuracy in κ_{c_1} stems from the shape of the N(p) order curve shown in Fig. 3, which has an infinite (or very steep) slope at the point $\kappa = \kappa_{c_1}$ where $M \to 0$. By contrast κ'_{c_1} was determined from the point where $\chi_p^{-1} \to 0$. Since the slope of the $\chi_p^{-1}(\kappa)$ curve becomes zero (or very small) at the point where it vanishes, the value of κ'_{c_1} had a much larger error, and in Ref. [11] we quoted a value $\kappa'_{c_1} \approx 0.24$, with no error estimate. The present analysis has enabled us to examine the lower phase boundary of the PVBC phase in more detail, and our best estimate for the *XXX* model is now $\kappa'_{c_1} \approx 0.28(2)$, as indicated in Fig. 5. The fact remains that the position of this phase boundary (i.e., the upper one for the tentative QSL phase) has the largest uncertainty of all those shown in Fig. 5, with a similar error along its length to that quoted above for the case $\Delta = 1$.

It is interesting to speculate whether the N(z) phase survives to higher values of the spin quantum number s than the $s = \frac{1}{2}$ case considered here. In this context we have performed some very preliminary low-order CCM SUB*m*–*m* calculations with $m \leqslant 8$ for the spin-1 version of the present *XX* model (i.e., with $\Delta = 0$). In the SUB*m*–*m* scheme one retains all multispin-flip configurations $\{I\}$ in the expansions of the CCM correlation operators S and $\tilde{S}$ involving no more than m single-spin flips spanning a range of m or fewer contiguous lattice sites. These preliminary SUB*m*–*m* calculations, based on both the N(p) and N-II(p) model states, exhibit three features: (a) the convergence of both E/N and M with increasing values of the truncation index m is more rapid than for the spin-$\frac{1}{2}$ model; (b) the energy curves for the N(p) and N-II(p) phases meet (or almost meet) near their respective termination points (so far only obtained rather approximately), and without any perceivable discontinuity in slope, at a value $\kappa \approx 0.25$; and (c) the corresponding extrapolated order parameters M of both the N(p) and N-II(p) phases appear to go to zero at values of κ very close to the same value $\kappa \approx 0.25$. These results alone show rather clearly that if, for the spin-1 model, there is a phase intermediate between the N(p) and N-II(p) phases, it can exist in only a very narrow region indeed around $\kappa \approx 0.25$. Finally, similar calculations based on the N(z) state for the spin-1 model show no signs of it providing a stable GS phase for any values of κ. Thus, our preliminary conclusion is that the stability of the N(z) phase is restricted to the spin-$\frac{1}{2}$ system, although more work would be needed to confirm this.

In conclusion, our CCM analysis gives a coherent picture of the full $T = 0$ GS phase diagram of the model under study. In particular, we have identified a candidate QSL regime, in which we have excluded magnetic or valence-bond forms of order. It would be of great interest to use other techniques in order to verify our findings.

We thank the University of Minnesota Supercomputing Institute for the grant of supercomputing facilities.

[1] E. Rastelli, A. Tassi, and L. Reatto, Physica B & C **97**, 1 (1979).
[2] J. B. Fouet, P. Sindzingre, and C. Lhuillier, Eur. Phys. J. B **20**, 241 (2001).
[3] A. Mulder, R. Ganesh, L. Capriotti, and A. Paramekanti, Phys. Rev. B **81**, 214419 (2010).
[4] R. Ganesh, D. N. Sheng, Y.-J. Kim, and A. Paramekanti, Phys. Rev. B **83**, 144414 (2011).
[5] B. K. Clark, D. A. Abanin, and S. L. Sondhi, Phys. Rev. Lett. **107**, 087204 (2011).
[6] A. F. Albuquerque, D. Schwandt, B. Hetényi, S. Capponi, M. Mambrini, and A. M. Läuchli, Phys. Rev. B **84**, 024406 (2011).
[7] H. Mosadeq, F. Shahbazi, and S. A. Jafari, J. Phys.: Condens. Matter **23**, 226006 (2011).
[8] J. Oitmaa and R. R. P. Singh, Phys. Rev. B **84**, 094424 (2011).
[9] F. Mezzacapo and M. Boninsegni, Phys. Rev. B **85**, 060402(R) (2012).
[10] P. H. Y. Li, R. F. Bishop, D. J. J. Farnell, and C. E. Campbell, Phys. Rev. B **86**, 144404 (2012).
[11] R. F. Bishop, P. H. Y. Li, D. J. J. Farnell, and C. E. Campbell, J. Phys.: Condens. Matter **24**, 236002 (2012).
[12] R. F. Bishop, P. H. Y. Li, and C. E. Campbell, J. Phys.: Condens. Matter **25**, 306002 (2013).
[13] R. Ganesh, J. van den Brink, and S. Nishimoto, Phys. Rev. Lett. **110**, 127203 (2013).
[14] Z. Zhu, D. A. Huse, and S. R. White, Phys. Rev. Lett. **110**, 127205 (2013).
[15] S.-S. Gong, D. N. Sheng, O. I. Motrunich, and M. P. A. Fisher, Phys. Rev. B **88**, 165138 (2013).
[16] X.-L. Yu, D.-Y. Liu, P. Li, and L.-J. Zou, Physica E **59**, 41 (2014).
[17] C. N. Varney, K. Sun, V. Galitski, and M. Rigol, Phys. Rev. Lett. **107**, 077201 (2011).
[18] C. N. Varney, K. Sun, V. Galitski, and M. Rigol, New J. Phys. **14**, 115028 (2012).
[19] Z. Zhu, D. A. Huse, and S. R. White, Phys. Rev. Lett. **111**, 257201 (2013).
[20] J. Carrasquilla, A. Di Ciolo, F. Becca, V. Galitski, and M. Rigol, Phys. Rev. B **88**, 241109(R) (2013).
[21] A. Di Ciolo, J. Carrasquilla, F. Becca, M. Rigol, and V. Galitski, Phys. Rev. B **89**, 094413 (2014).
[22] J. Oitmaa and R. R. P. Singh, Phys. Rev. B **89**, 104423 (2014).
[23] R. F. Bishop, P. H. Y. Li, and C. E. Campbell, Phys. Rev. B **89**, 214413 (2014).
[24] R. F. Bishop and H. G. Kümmel, Phys. Today **40**(3), 52 (1987).
[25] J. S. Arponen and R. F. Bishop, Ann. Phys. (NY) **207**, 171 (1991).
[26] R. F. Bishop, Theor. Chim. Acta **80**, 95 (1991).
[27] R. F. Bishop, in *Microscopic Quantum Many-Body Theories and Their Applications*, Lecture Notes in Physics Vol. 510, edited by J. Navarro and A. Polls (Springer-Verlag, Berlin, 1998), p. 1.
[28] R. F. Bishop, J. B. Parkinson, and Yang Xian, Phys. Rev. B **44**, 9425 (1991).
[29] C. Zeng, D. J. J. Farnell, and R. F. Bishop, J. Stat. Phys. **90**, 327 (1998).
[30] D. J. J. Farnell and R. F. Bishop, in *Quantum Magnetism*, Lecture Notes in Physics Vol. 645, edited by U. Schollwöck, J. Richter, D. J. J. Farnell, and R. F. Bishop (Springer-Verlag, Berlin, 2004), p. 307.
[31] R. F. Bishop, P. H. Y. Li, R. Darradi, J. Schulenburg, and J. Richter, Phys. Rev. B **78**, 054412 (2008).
[32] We use the program package CCCM of D. J. J. Farnell and J. Schulenburg; see http://www-e.uni-magdeburg.de/jschulen/ccm/index.html